Hindawi
Mobile Information Systems
Volume 2022, Article ID 4235419, 13 pages
https://doi.org/10.1155/2022/4235419

Research Article

Seismic Performance of New Fabricated Lightweight Herringbone Support Seismic Wall Based on ZigBee Sensor Technology

Xinjun Wang,[1] Honglin Yu,[2] and Chao Lu[3]

[1]*School of Urban Construction Chengdu Polytechnic, Chengdu, Sichuan, China*
[2]*Langfang D&G Machinery Technology Co., Ltd., Langfang, Hebei, China*
[3]*College of Mechanical Engineering, Chengdu University, Chengdu, Sichuan, China*

Correspondence should be addressed to Chao Lu; luchao@cdu.edu.cn

Received 27 January 2022; Revised 3 March 2022; Accepted 4 March 2022; Published 25 March 2022

Academic Editor: Hye-jin Kim

Reinforced concrete antiseismic wall structure has great load-bearing capacity and resistance to lateral displacement and is widely used as high-rise and super high-rise buildings. At present, in the seismic testing of buildings, the vibration signals that simulate earthquakes are transmitted through a wired transmission system for analysis after a certain amount of processing, and the seismic performance of the building is tested. The purpose of this paper is to analyze and study the seismic resistance of a newly fabricated lightweight herringbone braced seismic wall based on ZigBee sensor technology. In this paper, firstly, the research and exploration of the building seismic capability detection system using ZigBee technology wireless sensor are carried out, and the building seismic capability detection system is a wireless sensor network using ZigBee technology; it measures the seismic performance of the building by detecting the acceleration values of key parts in the building model. Then, the seismic design response spectrum is proposed, and the modal analysis is carried out at the same time, and the mode decomposition response spectrum method is given. Then, the seismic performance of the reasonable RC support lightweight herringbone support seismic wall was analyzed, and the seismic performance of the lightweight herringbone support structure was studied at the same time. The experimental results show that with the increase in the size of the RC support section, the bearing capacity and seismic performance of the lightweight herringbone support seismic wall are improved. The displacement ductility coefficient obtained is greater than 4, and the energy dissipation coefficient is 1.56, which meets the seismic requirements of the structure.

1. Introduction

At present, with the rapid and vigorous development of the socialist market economy, especially the deepening of the concept of sustainability, people are increasingly interested in the research of prefabricated concrete buildings with the advantages of low carbon, greening, environmental protection, and energy saving. At the same time, the fundamental reform of the construction methods of industrial and civil buildings not only implements the overall deployment of the rapid and vigorous development of architectural design industrialization and residential mechanization but also is an objective need to transform economic development methods and further improve the living conditions of residential and people's livelihoods. In recent years, from various ministries and agencies, to government departments, developers, and various research and development organizations including universities and colleges across the country, all of them have been exploring the development path of residential mechanization that is more suitable for actual national conditions. The industrialization of emerging materials has become an important part of the ideal development of the building materials industry and has been widely recognized and promoted in the field of urban engineering construction applications. Prefabricated building concrete structure itself, as a new industry booming building material structure form, naturally arouses people's attention.

The main structure of the prefabricated shear wall component is a fully prefabricated or semiprefabricated wall panel, which uses on-site installation or partial cast-in-place processing. It has the advantages of fast construction speed, fast production quality, environmental protection,

and promotion of sustainable economic and social development. Therefore, the research on prefabricated shear wall components is particularly important for the development of prefabricated structural systems. Although the reinforced concrete shear wall structure has good seismic resistance, it also has disadvantages such as complex construction technology, environment, and noise pollution; the self-weight of the traditional prefabricated shear wall brings great inconvenience to the hoisting during construction and increases the load of the structure and the seismic effect. Therefore, this article proposes a new type of lightweight herringbone support seismic wall, which can reduce the weight of the components by replacing the least stressed part of the wall with diagonal braces with a smaller cross-section.

According to the research progress at home and abroad, different scholars also have a certain degree of cooperation in ZigBee sensor and seismic performance: Alhmi Ed At T proposed a low-cost system architecture that has been proposed for automatic real-time monitoring of indoor air quality. The designed system is in the pilot phase, 4 sensor nodes are deployed in the indoor environment, more than 4 weeks of data have been collected, and performance analysis and evaluation have been carried out. The environmental data from the sensor node is sent through the ZigBee communication protocol. The system he proposed is low in cost and has achieved low power consumption. In addition to the actual deployment, he also introduced the hardware and network architecture [1]. Tian et al. designed a wireless network communication system based on ZigBee protocol by using CC2530 chip as processor and combining with front-end CC2530. The temperature and humidity data sent back by the main module receiving node will be sent to the host computer by the serial assistant. Then, the host computer receives and displays the data so that the user can check them easily [2]. In the remote monitoring of the structural integrity of the building through the intelligent wireless sensor network, And DS uses ZigBee as the wireless network and accelerometer as the sensor to monitor the health of the building structure. ZigBee is used to send the collected information to the receiver part in the receiver part, and another ZigBee receives the information and sends the data to the microcontroller [3]. Abey et al. discuss a method for improving the bridge seismic properties by using the "parameter-based impact factor" that was developed by factor theory. The factors considered in the factor analysis are longitudinal reinforcement percentage, concrete compressive strength, reinforcement yield strength, transverse tie spacing, and column height [4]. Yu et al. aim to study the seismic performance of RC short and long columns with welded stirrups. Through the low-circumferential horizontal load test of the specimen, the technical indicators of seismic energy such as wear mode, hysteresis curve, skeleton curve, ductility, energy consumption capacity, hardness decay, and hardness decay are analyzed with emphasis [5]. Arthi and Jaya compared the structural behavior of the prefabricated shear wall-diaphragm connection with the overall connection under seismic loads. The overall connection uses U-shaped rods to connect the shear wall and the slab, and the prefabricated connection uses positioning rods in two steps [6]. Ma et al. introduced the experimental and numerical study of a new hybrid structural system, which includes a RC frame and reinforced masonry walls. In general, in his investigation, there are four different connection methods between the frame and the reinforced masonry wall. The mathematical values provide accurate predictions of failure modes and cyclic response, but do not fully replicate the squeeze response due to the neglect of key-slip effects [7]. Çelik and Kamali study is aimed at increasing awareness of the technical characteristics of cold-formed steel members and the advantages of lightweight steel structures compared to reinforced concrete. To achieve this goal, a case study was carried out to compare the light steel structure and the reinforced concrete structure in detail from different perspectives [8]. The postfire mechanical properties of concrete are a set of important parameters in the analysis of structural behavior after fire. In this study, Romi et al. tested four lightweight self-compacting concrete mixes with different fillers. These tests are performed by considering the age of the sample [9]. However, these scientists cannot try to use ZigBee sensor technology to analyze and explore the seismic function of the newly assembled lightweight herringbone support seismic wall.

The innovations of this article are reflected in as follows: (1) This article analyzed and studied the building seismic capacity detection system based on ZigBee technology wireless sensor; (2) proposed the seismic design response spectrum and analyzes the seismic influence coefficient curve; (3) modal analysis was performed, which was the work of obtaining the vibration frequency and mode shape of a multi-degree-of-freedom linear system; (4) proposed the mode decomposition response spectrum method, that is, in the process of solving the multi-degree-of-freedom system, each mode that can construct a free vibration component was regarded as a coordinate system; and (5) analyzed and studied the seismic performance of reasonable RC support lightweight herringbone support seismic wall and lightweight herringbone support structure.

2. Experimental Method

2.1. Antivibration Detection System Based on ZigBee Wireless Sensor. In wireless sensor networks, data communication between network nodes requires corresponding wireless network protocols, including physical layer, medium access layer, network layer, application layer, and so on. Among the many traditional short-range wireless network communication protocols, it is difficult to find a technology that can meet the requirements of wireless sensors with low data rate, high fault tolerance, high security, and strong anti-interference ability. So the many characteristics of ZigBee technology make it the best choice for wireless sensor networks.

The seismic performance detection system of buildings uses ZigBee wireless sensor network to detect the seismic performance of buildings by measuring the acceleration values of key parts of the building model. Figure 1 shows the structure of the entire system.

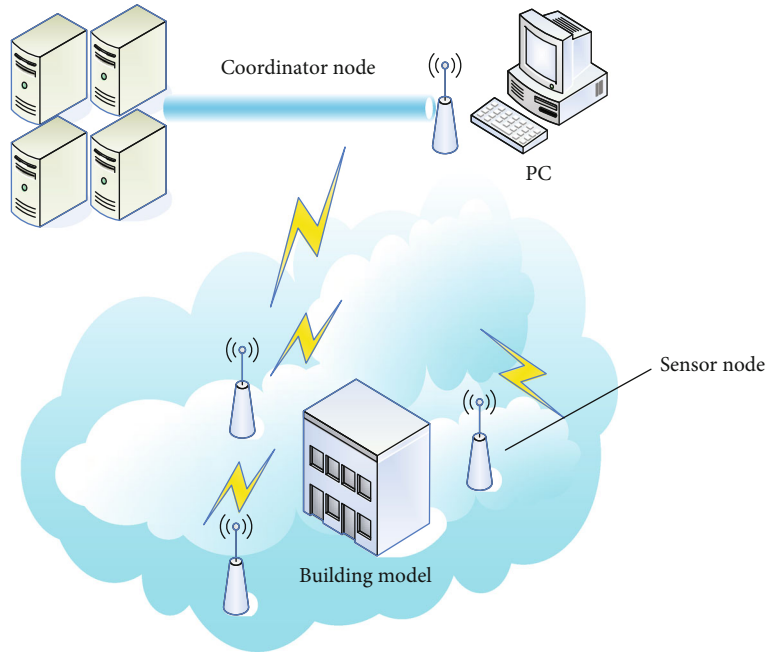

Figure 1: System structure diagram.

A number of sensor nodes are placed at the key stress points of the laboratory building model. These sensor nodes and the coordinator node form a short-distance miniature wireless sensor network to detect the seismic performance of the system. First, the coordinator node has established a website, and the sensor node can apply to enter this website. After successfully entering the network, the sensor node uses the acceleration sensor to start information processing on the acceleration value formed by the vibrating building model and uses the ZigBee radio frequency module to transmit the collected data to the coordinator node. Then, the coordinator node receives the data information and transmits the collected data information to the PC through RS-232 [10]. Figure 2 shows the basic structure diagram of the coordinator node. The coordinator node is mainly composed of processor module, ZigBee RF module, memory module, and power supply module [11].

The wireless media sensor network was constructed to form a star network, and the newly added nodes were reassigned network addresses [12]. Receiving the data collected by the acceleration sensor sent by the sensor node, complete the storage, analysis, and processing of the received data, and send the data to the PC via RS-232 to detect the seismic performance of the building [13]. Figure 3 shows the structure diagram of the wireless sensor network executive network system.

The coordinator node scans the wireless channel to form a wireless sensor network for detecting the vibration data of the building and stands by for the addition of new sensor nodes at any time [14]. After the sensor node successfully enters the network, the coordinator receives the data sent from the sensor node and uploads it to the PC via the RS-232 bus interface and then enters the idle state and waits for the next group of data [15]. Sensor nodes generally consist of data processor modules, ZigBee radio frequency transmission modules, sensor modules, and power supply modules [16].

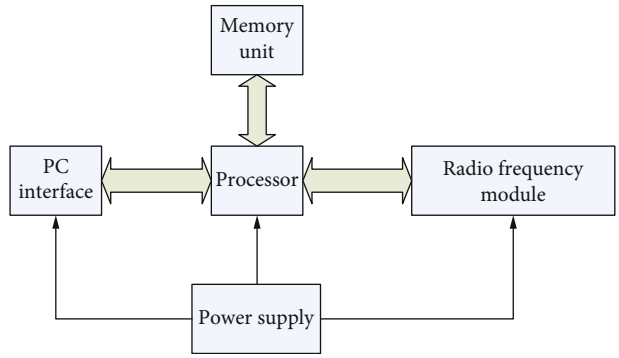

Figure 2: Basic structure diagram of the coordinator node.

The main functions of the sensor node are as follows: join the network established by the coordinator through the radio frequency module, use the acceleration sensor to complete the collection of building vibration signals, process the collected data, and use the method of direct communication with ZigBee to transmit the data to the coordinator node [17].

The sensor node applied to enter the network system, and the coordinator node responded to the application and assigned an Internet IP address to the sensor node. The sensor node successfully entered the network system [18]. When the vibration in the building is formed, the acceleration sensor is used to monitor the vibration message, and then, the information processor collects various data messages and transmits the collected various data messages to the coordination device through the radio frequency module [19].

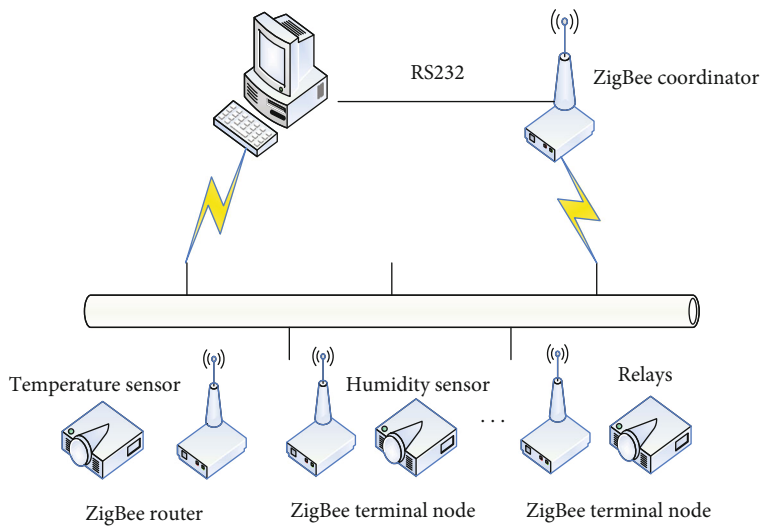

Figure 3: Wireless sensor network execution network system structure diagram.

The application prospect of ZigBee technology is very broad. In the next few years, ZigBee will have broad application prospects in many fields such as industrial control, industrial wireless positioning, home networking, automotive automation, building automation, consumer electronics, and medical equipment control. Especially home automation and industrial control will become the main application areas of ZigBee chips in the future. ZigBee technology fills up the gap in the wireless communication market with low cost, low power consumption, and low speed. The key to its success is rich and convenient applications. With the release of the official version of the agreement, more attention and research and development efforts will turn to application design and implementation, interconnection operability testing, and marketing. We have reason to believe that in the near future, more and more devices with built-in ZigBee functions will enter our lives, greatly improving our lifestyle and experience.

2.2. Response Spectrum of Seismic Design. For the system of a single degree-of-freedom, the mass point's absolute speed m can be expressed by the formula:

$$m = f_s(l) + f(l). \tag{1}$$

In the equation, $f_s(l)$ describes the acceleration wave of a given ground motion, and $f(l)$ refers to the acceleration rate of the system itself.

It is stipulated that the maximum absolute acceleration of the calculated mass point is

$$J_m = |m|_{\max}. \tag{2}$$

Then, the maximum seismic action that the structure can withstand during an earthquake is

$$P = kJ_m. \tag{3}$$

On the basis of a large number of calculations, we have introduced the concept of earthquake influence coefficient, namely

$$P = kJ_m = kd \bullet \frac{J_m}{d} = \frac{J_m}{d} \bullet D = \beta D. \tag{4}$$

Among them

$$m = \frac{J_m}{d} = |a_d|_{\max}, \tag{5}$$

where d is the seismic impact factor, which is calculated as the ratio of the horizontal seismic pressure applied to an elastic system with a single mass to the gravitational force of that mass.

The seismic influence coefficient curve is shown in Figure 4. That is, in the case of determining the damping ratio of the system, a special ground motion acceleration wave is determined after comprehensive selection of various factors such as site grouping and earthquake type. The earthquake influence coefficient a is only related to the natural vibration period R of the system [20–22].

2.3. Modal Analysis. Modal analysis is the work of obtaining the vibration frequency and mode shape of a multi-degree-of-freedom linear system. It is also the basis for solving the seismic response using the mode decomposition response spectrum method. Based on structural dynamics, the undamped free vibration equation can also be written as:

$$[D]\{\ddot{m}(r)\} + [H]\{m(r)\} = 0. \tag{6}$$

In the formula, $[D]$ is the mass matrix, $[H]$ is the structural stiffness matrix, and $\{\ddot{m}(r)\}$ and $\{m(r)\}$ construct the relative acceleration vector and position vector.

Taking the degree of freedom mode of the structure as the generalized coordinate system and according to the

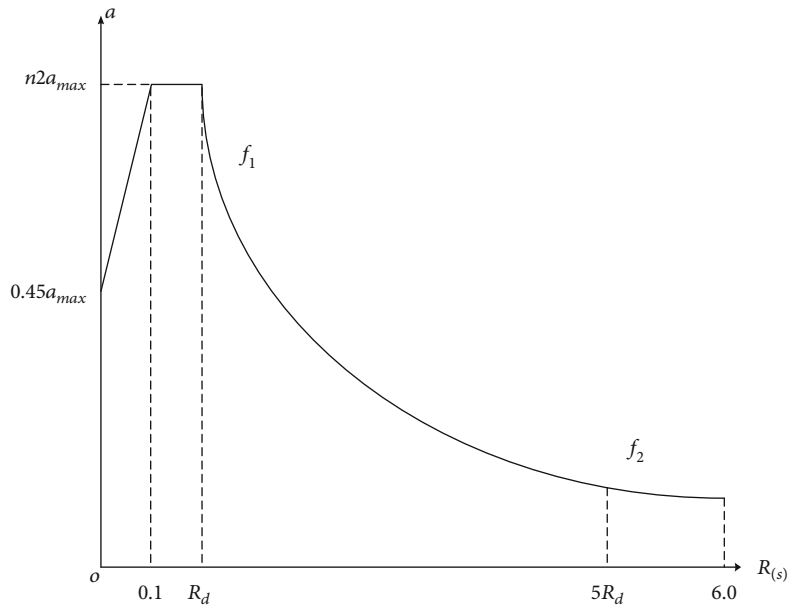

Figure 4: Earthquake influence coefficient curve.

nonzero solution of the free vibration equation, the frequency equation can be obtained as follows:

$$[H]\{M_g\} = v_g^2[D]\{M_g\}. \tag{7}$$

In the equation, v_g is the circumference of the g-th mode, and $\{M_g\}$ is the g-th mode vector.

Then, the period R_g of the g-th mode of the structure can be expressed by the following equation:

$$R_g = \frac{2\pi}{v_g}. \tag{8}$$

Therefore, to convert the calculation of natural vibration stage and mode shape into characteristic value and characteristic stage calculation, people generally choose the following methods to solve the building structure: (1) The iterative method is to transform the stiffness matrix into a flexibility matrix, perform mathematical processing on it, and then transform it into a variable eigenvalue calculation problem at different levels. Through this method, the first-order natural vibration order and the corresponding vibration mode can be obtained. (2) The Jacobian method of real symmetric matrix can calculate all vibration modes and periods. The method used is the subspace iteration method of the MIDAS/Gen software itself. This method incorporates the advantages of the iterative and Jacobi methods. The subspace adopts the generalized Jacobian method, and the iterative method is adopted between the subspaces, which has the advantages of high accuracy and short calculation time.

2.4. Mode Decomposition Response Spectrum Method. The definition of "modal decomposition" is that in the process of solving a multi-degree-of-freedom system, each mode that can construct a free vibration component is regarded as a coordinate system, and the movement of the component is regarded as vibration linear form of type:

$$\{m(r)\} = \sum_{g=1}^{d} p_g(r)\{M\}_g. \tag{9}$$

In the equation, $m(r)$ is the movement vector of the structure, $p_g(r)$ is the generalized displacement coordinate of the g mode, and $\{M\}_g$ is the g-th mode of the system.

In the same way, the inertial motion can be expanded like the mode shape. Using the orthogonal nature of the mode shape, the equilibrium equation about the generalized coordinates can be obtained:

$$p_g(r) + 2\varphi_g v_g p_g(r) + v_g^2 p_g(r) = -\beta_g \ddot{m}(r), \tag{10}$$

$$\beta_g = \frac{\{M\}_g^R[D]\{E\}}{\{M\}_g^R[D]\{M\}_g} = \frac{\sum_{b=1}^{c} d_b D_{gb}}{\sum_{b=1}^{c} d_b D_{gb}^2}. \tag{11}$$

In the equation, φ_g is the damping ratio of the g mode, v_g is the circular frequency ratio of the g mode, and β_g is the participation coefficient of the g mode; it represents the proportion of the g mode in inertial motion per unit time, which satisfies:

$$\sum_{g=1}^{c} \beta_g M_{gb} = 1. \tag{12}$$

$\ddot{m}(r)$ is the acceleration of ground motion, d_b is the mass of the b-th particle.

Introducing $\Delta_g(r)$ as the displacement response of a single-degree-of-freedom system with a damping ratio of φ_g

and a natural frequency of v_g, the solution of the g-th mode of equation (10) can be expressed as

$$p_g = \beta_g \Delta_g(r). \tag{13}$$

Then, the shift reaction of the b-th prime is

$$m_b(r) = \sum_{g=1}^{c} p_g(r) M_{gb} = \sum_{g=1}^{c} \beta_g \Delta_g(r) M_{gb}. \tag{14}$$

The horizontal seismic force of a multi-degree-of-freedom system can also be represented by the inertial force of the point body. The horizontal seismic force on the particle b is

$$Y_b(t) = -d_b \bullet [\ddot{m}_d(r) + \ddot{m}_b(r)]. \tag{15}$$

In the equation, $\ddot{m}_b(r)$ represents the relative acceleration of the mass point b.

From equation (14), equation (15) can be written as:

$$\begin{aligned} Y_b(t) &= -d_b \bullet [\ddot{m}_d(r) + \ddot{m}_b(r)] \\ &= -m \bullet \left[\sum_{g=1}^{c} \ddot{m}_d(r) \beta_g M_{gb} + \sum_{g=1}^{c} \beta_g \ddot{\Delta}_g(r) M_{gb} \right] \\ &= \sum_{g=1}^{c} Y_{gb}(t), \end{aligned} \tag{16}$$

$$Y_{gb}(t) = -d_b \beta_g M_{gb} \left[\ddot{m}_d(r) + \ddot{\Delta}_g(r) \right]. \tag{17}$$

Equation (16) can be used to obtain the horizontal seismic effect of particle b and its variation with time, and the maximum value can be obtained. A simpler way is to use the response spectrum of a single degree of freedom system. According to equation (17), the maximum horizontal seismic effect of each particle in the g mode and the interaction effect produced by it can be synthesized, and then, the effect of the multi-degree-of-freedom system under the maximum horizontal seismic interaction can be obtained.

Equation (17) can be written as:

$$Y_{gb_{\max}} = \left| \frac{\ddot{m}_d(r) + \ddot{\Delta}_g(r)}{d} \right|_{\max} D_b \beta_g M_{gb}. \tag{18}$$

In the above equation, let $\mu_g = |(\ddot{m}_d(r) + \ddot{\Delta}_g(r))/d|_{\max}$, μ_g be the seismic influence coefficient of a single-degree-of-freedom system with the g-mode natural vibration time of $R_g = 2\pi/v_g$, so that the maximum seismic influence on the g-th mode particle b can be obtained as

$$Y_{gb_{\max}} = \mu_g \beta_g M_{gb} D_b. \tag{19}$$

The seismic influence coefficient is determined by the seismic design response spectrum to obtain the maximum seismic influence of a certain mode shape on each particle, thereby converting the dynamic problem into a static problem. According to the static solution, the maximum seismic effect of each mode shape can be obtained. According to the understanding of random vibration, the ground motion in the process of earthquake damage is considered to be a stable random process. Therefore, the total maximum seismic action effect T formed by the translational vibration mode of the structure at a certain position can be approximately determined by the "sum of squares" method, namely

$$T = \sqrt{\sum_{g=1}^{b} T_g^2}. \tag{20}$$

3. Analysis of Results

3.1. Seismic Characteristics of Lightweight Herringbone-Supported Seismic Wall with Reasonable RC Support. Studies have shown that the size of the opening has a great influence on the seismic performance of the lightweight herringbone support seismic wall. Another important factor is the RC support. On the basis of determining the optimal size of the opening, the section size and section reinforcement of the support were changed, respectively, and their influence on the seismic performance of the lightweight herringbone support seismic wall was studied, so as to determine a reasonable RC support.

Figure 5 shows the skeleton curve obtained when changing the size of the RC support section, and Table 1 shows the relevant characteristic values obtained by changing the section size of the RC support. From this figure and the table, it can be seen that the stiffness, bearing strength, and seismic performance of the lightweight herringbone braced seismic wall increase with the increase of the cross-sectional size of the RC brace.

Figure 6 shows related seismic performance indicators such as the elastic interlayer displacement angle, the elastic-plastic interlayer displacement angle, the ductility coefficient, and the energy dissipation coefficient. It can be observed that the ductility and energy dissipation coefficients increase as the cross-sectional size of the support increases; when the size of the support section is 200×300, its ultimate bearing capacity is slightly smaller than that of the solid seismic wall, but the degree of decrease does not exceed 5%.

Figure 7 shows the skeleton curve obtained when the reinforcement of the RC support section is changed, and Figure 8 shows the relevant characteristic values obtained by changing the reinforcement of the RC support section. From this figure, it can be seen that the bearing capacity of the lightweight herringbone braced seismic wall increases with the increase of the RC bracing cross-sectional reinforcement.

Figure 9 shows related seismic performance indexes such as the displacement angle between elastic layers, the displacement angle between elastic and plastic layers, the ductility coefficient, and the energy dissipation coefficient. It is observed that the consumption coefficient increases and the ductility coefficient increases slightly as the reinforcement of the support section increases; when the

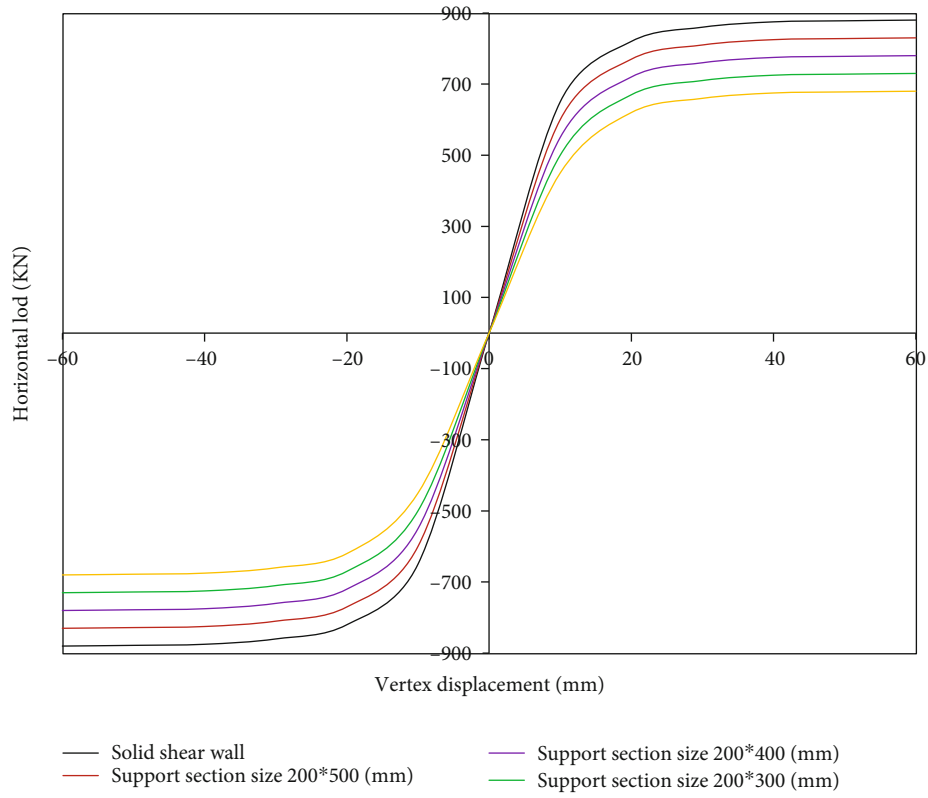

Figure 5: Skeleton curve obtained by changing the size of the support section.

Table 1: Relevant characteristic values obtained by changing the size of the support section.

Lightweight herringbone support seismic wall	Fracture points		Earnings point		Peak point		Point of destruction	
	Fcr	cr	Fy	y	Fm	m	Fu	u
Solid seismic wall	449	2.1	721	5.8	851	17.8	723	36.1
Support section size 200*200	239	1.7	551	9.7	749	29.1	641	37.9
Support section size 200*300	291	2.0	598	10.1	811	30.2	692	45.2
Support section size 200*400	319	2.0	658	10.1	859	28.3	728	53.8

supporting section reinforcement is 6#12, its ultimate bearing capacity is slightly lower than that of the solid seismic wall; the obtained displacement angle of the ductile interlayer is less than 1/800, and the displacement angle of the elasto-plastic interlayer is less than 1/100, which meets the deformation check calculation under seismic action; the displacement ductility coefficient is greater than 4, and the energy dissipation coefficient is 1.56, which meets the seismic requirements of the structure.

3.2. Seismic Performance Analysis of Lightweight Herringbone Support Structure. When an earthquake occurs, the structure will be subjected to force; that is, the seismic load acts on the building structure, which causes the deformation and destruction of the structure. Under the action of two-way earthquake load, the deformation and failure of the structure are obviously stronger than that of one-way earthquake. For a plane L-shaped structure, its mass and stiffness distribution are asymmetrical. Therefore, when discussing the causes of horizontal seismic loads, the torsion causes under the condition of two-way horizontal epicenters should be considered. That is, the response spectrum analysis is carried out in the X direction and the Y direction, respectively, and the earthquake damage is fully studied to ensure the safety of the structure in the case of earthquake damage. Using the SAP2000 software, the response spectra of the original basic model, the herringbone support, and the X-shaped support structure in the X and Y directions were analyzed.

When determining the seismic influence coefficient, many factors need to be considered, such as the damping ratio and self-excited vibration period of the building structure, the seismic fortification intensity of the area where the building components belong, and the design seismic grouping, including the site category of the area, will affect the determination of the coefficient.

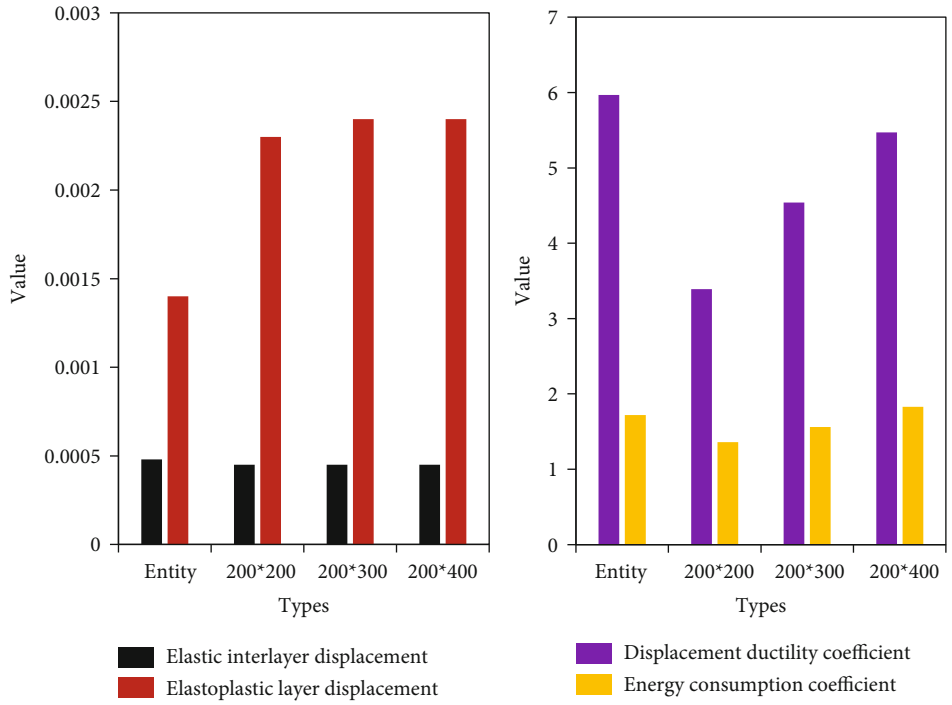

Figure 6: Related seismic performance indicators.

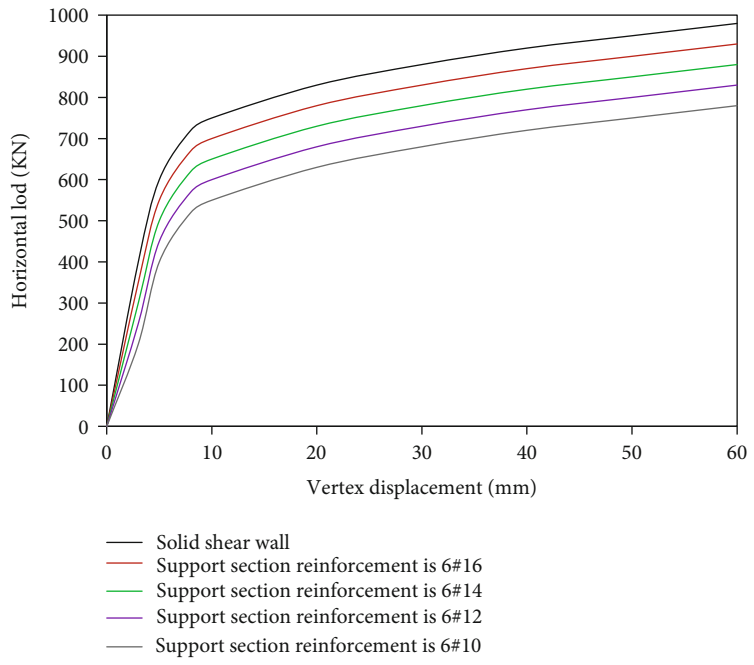

Figure 7: Skeleton curve obtained by changing the supporting gluten.

In the SAP2000 software, the program cannot provide data about floor displacement. In the actual research and analysis process, the displacement of the structural floor under the action of the earthquake is replaced by the displacement of the node. Under the action of two-way earthquake, due to the existence of seismic force, the collection and summary of structural displacement data are obtained. As shown in the table, combined with the known story height values, it is easy to obtain the displacement angle between stories. Table 2 shows the variation of interstory discharge and interstory discharge corner when the structure is unsupported under earthquake action. Table 3 shows the variation of interstory discharge and interstory discharge corner of the X-supported structure under earthquake action.

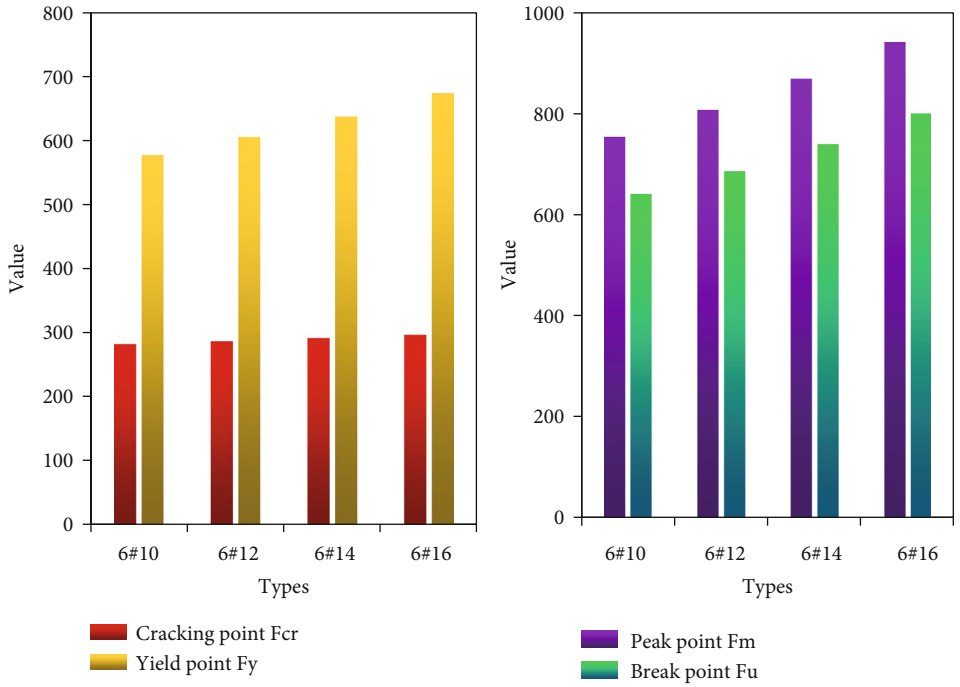

Figure 8: Relevant characteristic values obtained by changing the reinforcement of the support section.

In the SAP2000 software, the program cannot provide data for the displacement of the floor. In our actual research and analysis process, the displacement of the structural floor under the earthquake is replaced by the displacement of a node, as shown in Table 4.

We analyzed the state of the structure under the action of two-way earthquakes. For the basic model, the displacement in the X direction of the first layer of model 1 is 2.8431, the displacement in the Y direction is 2.3777, the maximum lateral displacement is 14.9763, and the maximum longitudinal displacement is 13.4607. By comparing the lateral and longitudinal displacements of each floor, it is found that the displacement in the X direction is always higher than the displacement in the Y direction. Model 2 and Model 3 have the same situation under the two different supports. This means that the lateral displacement resistance of the structure in the X direction is lower than the lateral displacement resistance in the Y direction. Figure 10 shows the maximum displacement changes in the lateral (a) and longitudinal (b) directions of the structure under the action of two-way earthquakes.

The maximum interlayer displacement of the model is analyzed and calculated. Under the action of two-way earthquakes and mainly X-direction earthquakes, it was found that the maximum interlayer displacement of model 1 in the X-direction appeared on the third layer, with a displacement of 3.3934 mm. The maximum interlayer displacements of model 2 and model 3 are also the same, with specific dimensions of 3.3307 mm and 3.1095 mm, respectively. Under the action of two-way earthquakes, the Y-direction earthquakes dominate. It is not difficult to see that the Y -direction trend is consistent; that is, the maximum value appears on the third layer. The calculated maximum interlayer displacements of the three models are 4.2232 mm, 2.4106 mm, and 2.3449 mm, respectively. For the floor with the largest structural displacement, when an earthquake occurs, the structure may be damaged at that location, which should be considered in the design stage. Antiseismic measures must be taken, such as increasing the cross-sectional area of the component or increasing the lateral force resistance of the floor slab to avoid damage.

Comparing the displacement of model 1 without support, model 2 with X-shaped support, and model 3 with herringbone center support, it is found that under the action of the support rods, the maximum lateral displacement of the structure is reduced from 15.2763 mm to 13.1528 mm and 11.9465, and the maximum longitudinal displacement is reduced from 13.4593 mm to 10.5295 mm and 9.7627 mm, respectively. It shows that the support rod effectively improves the rigidity of the structure and plays a significant role in maintaining the overall stability of the structure under the action of an earthquake. The displacement reduction range of the two different supports is also different, and the displacement reduction range of the herringbone center support is larger. Under the analysis model in this paper, the lateral rigidity of the herringbone central support structure is greater than that of the X-shaped central support structure, and its seismic performance is better under seismic loads.

4. Discussion

This article mainly describes a new type of fabricated lightweight herringbone support seismic wall technology; it is in the category of manufacturing design and construction technology of prefabricated concrete components and can

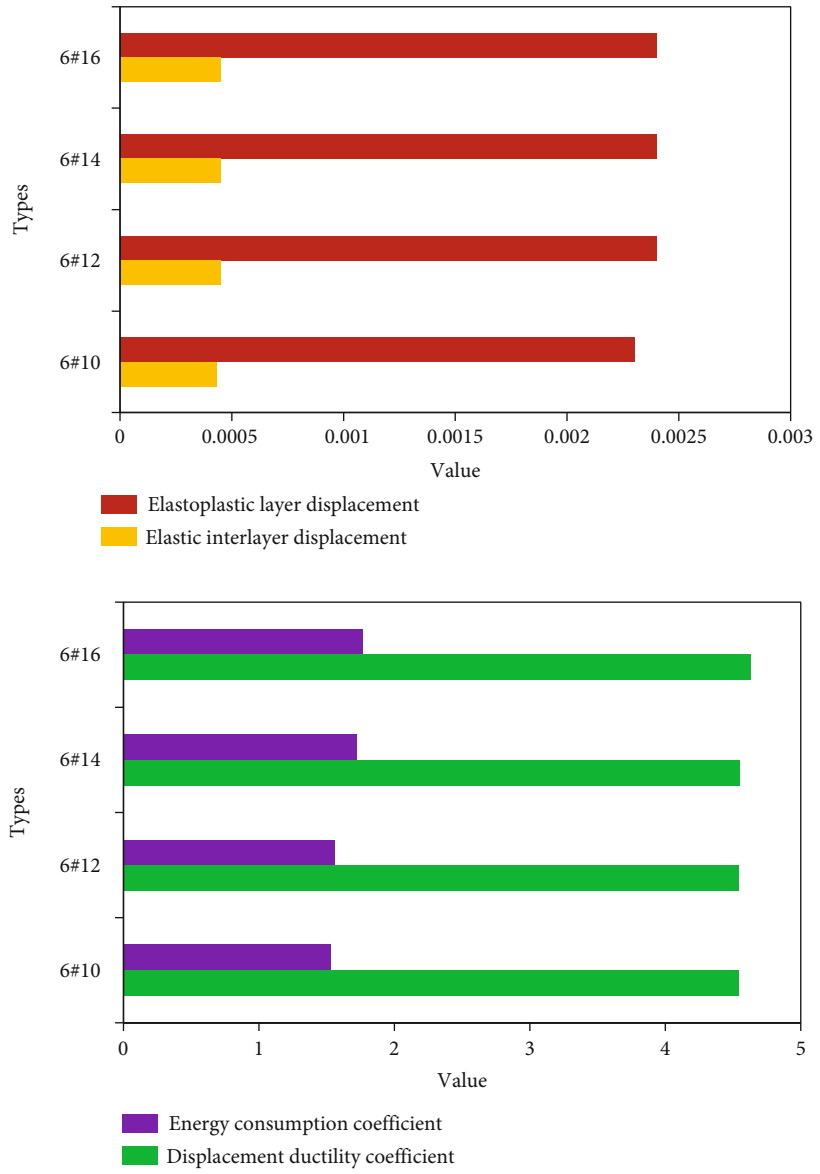

Figure 9: Related seismic performance indicators.

Table 2: Interstory displacement and interstory displacement angle without supporting structure under earthquake action.

Floor	Two-way earthquake action			
	Floor lateral displacement (mm)	Displacement angle between floors (rad)	Floor longitudinal displacement (mm)	Displacement angle between floors (rad)
1	2.7982	1/998	2.1986	1/1339
2	5.9789	1/897	5.3895	1/938
3	9.4976	1/891	8.5968	1/929
4	12.7015	1/961	10.9873	1/1139
5	14.9763	1/1201	13.4607	1/1372

be applied to solve the problems of traditional seismic wall self-weight and complex construction technology, which is conducive to the development and promotion of the process of building industrialization. Each piece of assembled lightweight herringbone support seismic wall is an integral prefabricated component formed by opening a hole in the middle part of the solid shear wall and adding herringbone support, in which the joints of the wall body are made of teeth. When the vertical connection between the upper and lower walls is carried out, the joint method of mechanical

Table 3: Interlayer displacement and interlayer displacement angle of X-shaped supporting structure under earthquake action.

Floor	Two-way earthquake action			
	Floor lateral displacement (mm)	Displacement angle between floors (rad)	Floor longitudinal displacement (mm)	Displacement angle between floors (rad)
1	2.2013	1/1402	1.7946	1/1589
2	5.0978	1/989	3.9867	1/1304
3	8.5102	1/892	6.9021	1/1251
4	11.0215	1/1198	8.9023	1/1329
5	12.9879	1/1297	10.4972	1/7802

Table 4: Interstory displacement and interstory displacement angle of a herringbone support structure under earthquake action.

Floor	Two-way earthquake action			
	Floor lateral displacement (mm)	Displacement angle between floors (rad)	Floor longitudinal displacement (mm)	Displacement angle between floors (rad)
1	1.9859	1/1501	1.5989	1/1839
2	4.7001	1/1089	4.0023	1/1328
3	7.8031	1/971	5.9789	1/1301
4	9.8978	1/1402	7.0982	1/1604
5	12.005	1/1497	9.8028	1/1862

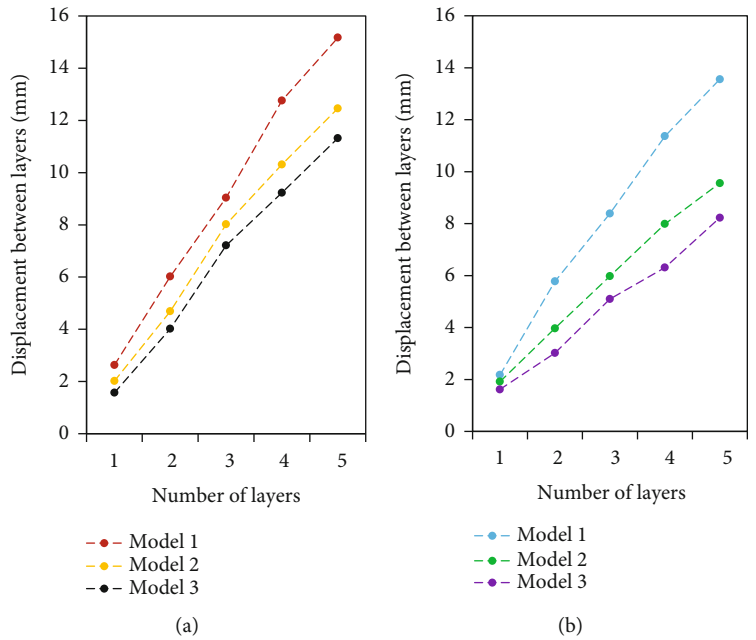

Figure 10: The maximum displacement of the structure in the lateral (a) and longitudinal (b) directions under the action of two-way earthquakes.

connection or welding connection shall be adopted for the joints of the steel bars, and the joints shall be filled by the method of injecting cement mortar. At the junction of the upper and lower earthquake-proof walls, the wall surface should be made into a "convex" shape with tongue and groove, and the height of the protrusion in the middle should not be less than 1/2 the thickness of the floor, retract the length of floor slab, roof slab, and shelf with a height of not less than 60 mm to both ends (both sides of the internal seismic wall need to shrink inward, and the inner side of the external seismic wall needs to shrink inward).

5. Conclusions

When analyzing the seismic performance of the RC-supported lightweight herringbone-supported seismic wall,

the size of the RC support section of the lightweight herringbone support seismic wall is 200 × 300 (mm), and when the reinforcement of the support section is 6#12 (mm), its seismic performance is basically the same as that of a solid shear wall. When analyzing the seismic performance of the lightweight herringbone support structure, the structure was subjected to two-way seismic action, and the displacement of the structure under the seismic action met the relevant mandatory requirements of the seismic code, indicating that the light steel structure has good seismic performance. After adding the herringbone and X-shaped center supports to the original structure, the lateral and longitudinal displacements of the structure are smaller than those of the original model. The support has a significant effect on reducing structural deformation, and the addition of herringbone supports will reduce the displacement to a greater extent. In this paper, the seismic performance of the proposed prefabricated lightweight herringbone support seismic wall is numerically simulated and analyzed, but there are still many shortcomings, and further research is needed. When analyzing and researching the seismic performance of the prefabricated lightweight herringbone support seismic wall, due to many influencing factors, the interaction between the various factors may not be fully considered.

Data Availability

The data used to support the findings of this study are available from the corresponding author upon request.

Conflicts of Interest

The authors declare no conflicts of interest.

Acknowledgments

This research study is sponsored by the Department of Public Service, China Earthquake Administration, Special Research Project (2021) on Public Services for Earthquake Prevention and Disaster Mitigation Key Project. The project number is dzjgfs2021006. The authors thank the project for supporting this article.

References

[1] T. Alhmiedat and G. Samara, "A low cost ZigBee sensor network architecture for indoor air quality monitoring," *International Journal of Computer Science & Information Security*, vol. 15, no. 1, pp. 140–144, 2017.

[2] X. Tian, J. Li, and L. Luo, "Design of greenhouse temperature and humidity measuring system based on ZigBee technology," *Computer Systems Science & Engineering*, vol. 33, no. 5, pp. 317–326, 2018.

[3] D. S. And and G. Maheshkumar, "Wireless mems-based accelerometer sensor system for structure vibration and post defamation monitoring," *Advances in computational sciences and technology*, vol. 10, no. 11, pp. 3197–3204, 2017.

[4] E. T. Abey, T. P. Somasundaran, and A. S. Sajith, "Study on seismic performance enhancement in bridges based on factorial analysis," *Earthquake Engineering & Engineering Vibration*, vol. 16, no. 1, pp. 181–198, 2017.

[5] Y. Yu, Z. Dang, Y. Yang, Y. Chen, and H. Li, "Seismic performance of RC columns with full resistance spot welding stirrups," *Structural Engineering and Mechanics*, vol. 73, no. 5, pp. 543–554, 2020.

[6] S. Arthi and K. P. Jaya, "Seismic performance of precast shear wall-slab connection under cyclic loading: experimental test vs. numerical analysis," *Earthquake Engineering and Engineering Vibration*, vol. 19, no. 3, pp. 739–757, 2020.

[7] X. Ma, J. Ma, and Y. Yue, "Experimental and numerical investigation on seismic performance of a hybrid RC frame system with stiffened masonry wall," *Journal of Advanced Concrete Technology*, vol. 16, no. 12, pp. 600–614, 2018.

[8] T. Çelik and S. Kamali, "Multidimensional comparison of lightweight steel and reinforced concrete structures: a case study," *Tehnicki Vjesnik*, vol. 25, no. 4, pp. 1234–1242, 2018.

[9] A. Romi and S. Juradin, "Influence of mixture design, age, and cooling regime on post-fire mechanical properties of lightweight self-compacted concrete," *Elektronički časopis građevinskog fakulteta Osijek*, vol. 11, no. 20, pp. 1–12, 2020.

[10] A. Narmada and P. S. Rao, "Performance of IP-based wireless sensor network with Cartesian terrain," *Research Journal of Engineering and Technology*, vol. 8, no. 3, pp. 219–224, 2017.

[11] L. B. Fargier-Gabaldón, "Boundary elements in rectangular walls for earthquake resistance," *Concrete International*, vol. 40, no. 9, pp. 43–45, 2018.

[12] K. Mrozek, "Simulation study of induction heating of multimetallic injection moulds," *Journal of Simulation Modelling*, vol. 17, no. 2, pp. 220–230, 2018.

[13] H. Nakazawa, T. Hara, D. Suetsugu et al., "Experimental evaluation on earthquake-resistance of road retaining wall using gabion," *Journal of Disaster Research*, vol. 13, no. 5, pp. 897–916, 2018.

[14] L. J. Vinnell, J. Mcclure, and T. L. Milfont, "Do framing messages increase support for earthquake legislation?," *Disaster Prevention & Management*, vol. 26, no. 1, pp. 28–40, 2017.

[15] I. Kongar, S. Giovinazzi, and T. Rossetto, "Seismic performance of buried electrical cables: evidence-based repair rates and fragility functions," *Bulletin of Earthquake Engineering*, vol. 15, no. 7, pp. 3151–3181, 2017.

[16] H. Moniri, "Evaluation of seismic performance of reinforced concrete (RC) buildings under near-field earthquakes," *International Journal of Advanced Structural Engineering*, vol. 9, no. 1, pp. 13–25, 2017.

[17] S. Momenzadeh, M. T. Kazemi, and M. H. Asl, "Seismic performance of reduced web section moment connections," *International Journal of Steel Structures*, vol. 17, no. 2, pp. 413–425, 2017.

[18] E. Yooprasertchai and P. Warnitchai, "Seismic performance of precast hybrid moment-resisting frame/rocking wall systems," *Magazine of Concrete Research*, vol. 70, no. 21-22, pp. 1118–1134, 2018.

[19] C. Zeris, A. Lalas, and E. Spacone, "Performance of torsionally eccentric RC wall frame buildings designed to DDBD under bi-directional seismic excitation," *Bulletin of Earthquake Engineering*, vol. 18, no. 7, pp. 3137–3165, 2020.

[20] W. Zhou, Y. Liu, and W. Zheng, "Seismic performance of self-centering concrete shear wall: state-of-the-art review and prospects," *Harbin Gongye Daxue Xuebao/Journal of Harbin Institute of Technology*, vol. 50, no. 12, pp. 1–13, 2018.

[21] T. Lin, P. Wu, F. M. Gao, and T. S. Wu, "Energy-saving cloud workflow scheduling based on optimistic cost table," *International Journal of Simulation Modelling*, vol. 19, no. 3, pp. 505–516, 2020.

[22] Q. Cao, Y. Bao, and Y. Shen, "Effect of core hole size on seismic performance of high rise frame concrete lattice wall structure," *Liaoning Gongcheng Jishu Daxue Xuebao (Ziran Kexue Ban)/ Journal of Liaoning Technical University (Natural Science Edition)*, vol. 37, pp. 70–74, 2018.